Carnahan, N. F. and K. E. Starling, "Intermolecular Repulsions and the Equation of State for Fluids," *AIChE J.*, **18**, 1184-1189 (1972).
Chandler, D., "Structures of Molecular Liquids," *Ann. Rev. Phys. Chem.*, **29**, 441-71 (1978).
Chueh, P. L. and J. M. Prausnitz, "Vapor-Liquid Equilibria at High Pressures. Vapor-Phase Fugacity Coefficients in Non-Polar and Quantum-Gas Mixtures," *Ind. and Eng. Chem. Fund.*, **6**, 492 (1967).
Diepen, G. A. and F. E. Scheffer, "The Solubility of Naphthalene in Supercritical Ethylene," *J. Amer. Chem. Soc.*, **70**, 4085-4090 (1948).
Diepen, G. A. and F. E. Scheffer, "The Solubility of Naphthalene in Supercritical Ethylene II," *J. Phys. Chem.*, **57**, 575-577 (1953).
Din, F., *Thermodynamic Function of Gases*, **2**, Butterworths, London (1962).
Gangoli, N. and G. Thodos, "Liquid Fuels and Chemical Feedstocks from Coal by Supercritical Gas Extraction," *Ind. Eng. Chem. Prod. Res. Dev.*, **16**, 208-216 (1977).
Gearhart, J. A., and L. Garwin, "A New Economical Approach to Residuum Processing," NPRA Annual Meeting, AM-76-36 (March 30, 1976).
Johnston, K. P., "High-Pressure Phase Equilibria: The Solubility of Non-Volatile Molecules in Supercritical Fluids," M.S. Thesis, University of Illinois, Urbana, IL (1979).
Kaul, B. K. and J. M. Prausnitz, "Second Virial Coefficients of Gas Mixtures Containing Simple Fluids and Heavy Hydrocarbons," *Ind. Eng. Chem. Fundam.*, **16**, 335-340 (1977).
Mackay, M. E. and M. E. Paulaitis, "Solid Solubilities of Heavy Hydrocarbons in Supercritical Solvents," *Ind. Eng. Chem. Fundam.*, **18**, 149-153 (1979).
Oellrich, L. R., H. Knapp, and J. M. Prausnitz, "A Simple Perturbed Hard-Sphere Equation of State Applicable to Subcritical and Supercritical Temperatures," *Fluid Phase Equilibria*, **2**, 163-171 (1978).
Tsekhanskaya, Y. V., M. B. Iomtev, and E. V. Mushkina, "Solubility of Naphthalene in Ethylene and Carbon Dioxide Under Pressure," *Russ. J. Phys. Chem.*, **38**, 1173-1176 (1965).
Vera, J. H. and J. M. Prausnitz, "Generalized van der Waals Theory for Dense Fluids," *Chem. Eng. J.*, **3**, 1-13 (1972).
Zosel, K., "Separation with Supercritical Gases: Practical Applications," *Ang. Chemie Int. Ed.*, **17**, 702-709 (1978).

Manuscript received June 12, 1980; revision received October 30, and accepted November 21, 1980.

Studies in the Synthesis of Control Structures for Chemical Processes

YAMAN ARKUN
and
GEORGE STEPHANOPOULOS
Department of Chemical Engineering and Materials Science
University of Minnesota
Minneapolis, MN 55455

Part V: Design of Steady-State Optimizing Control Structures for Integrated Chemical Plants

This paper addresses the question of how to design the steady-state optimizing control system for a large scale interconnected chemical plant. The integrated design approach is structured within the framework of the hierarchical control theory and is based on the concepts of constraint control, hierarchical decomposition and nonlinear mathematical programming. Theoretical developments lead to the generation of alternative operational policies of practical value. An imbedded branch and bound screening strategy is given to select the best policy, which will be implemented on-line by the optimizing plant controllers. The general design approach has the broad applicability to any interconnected large scale system, and its application is demonstrated on a gasoline polymerization plant.

SCOPE

Process control tasks for a chemical plant consist of certain *regulatory* (i.e., product quality control, safety, environmental regulations, material balance control, etc.) and *economic* (i.e., most profitable steady-state plant operation) objectives, which have to be satisfied in the presence of a wide variety of plant disturbances. Typical disturbances are: changing raw material properties, different product specifications, varying market demands, fluctuating prices of raw materials and energy and many other external changes (e.g., ambient conditions, temperature drifts, pressure and flowrate changes, etc.). Classification of control objectives into two such categories formulates the different activities involved during the design of the regulatory and optimizing control structures. For further details on control tasks, the reader is referred to Morari, Arkun and Stephanopoulos (1980a).

In the last decade, extensive research has been conducted on the synthesis of process control structures (Govind and Powers,

Mr. Arkun is presently with the Department of Chemical and Environmental Engineering, Rensselaer Polytechnic Institute, Troy, NY 12181.
Parts I, II, and III of this paper appeared in *AIChE J.*, **26**, 220-260 (1980), and Part IV was published in *AIChE J.*, **26**, 975 (1980).

1976; Douglas, 1977; Morari and Stephanopoulos, 1980b,c; Umeda et al., 1978) with mostly regulatory objectives in mind, i.e., to keep certain variables at specified set-points. Furthermore, escalating energy costs, scarce and expensive raw materials have reinforced the need to operate chemical plants in the most profitable fashion over a wide spectrum of operating conditions. According to recent industrial viewpoint articles (Latour, 1976; Ellingsen, 1976; Barkelew, 1976; Lee and Weekman, 1976), economic incentives, which were harder to justify or implement on-line in the past, now call for new methodologies for the design of optimizing control systems and their practical implementational strategies.

In this paper, we will characterize the optimizing control system by a set of plant controllers which exercise in real time certain control activities with the purpose of achieving and preserving an optimal economic plant performance. As the plant disturbances change, optimal set-point values for the controllers will have to be determined and the necessary set-point changes will have to be implemented on-line. In contrast to the flourishing research works on the design of regulatory control structures, there has been no systematic approach towards the design and implementation of such optimizing control systems for complete plants.

In the Part IV of this series (Arkun and Stephanopoulos, 1980), we have presented a rigorous design approach for the optimizing control of single unit operations (e.g., distillation column reactor, etc.). In this paper, we are interested in the optimizing control of large-scale chemical plants composed of a large number of interconnected and interacting process units. The large dimensionality and the interaction of units with each other make the plant control a challenging and overwhelming task with many generic problems which are not encountered in the optimizing control of single unit operations.

Any approach towards the design of optimizing control systems for large-scale plants becomes unduly complicated and lacks practical appeal unless decomposition aspects are included. Our design methodology will utilize the dual hierarchical decomposition concepts (i.e., decomposition of the process into subsystems—multiechelon structure, and decomposition of the control tasks—multilayer structure) which provide the appropriate tool for rigorous and practically acceptable designs. Within the general framework, we can rigorously formulate the interactions among interconnected units and the related optimizing control problems which are to be addressed during design. In the first part of this paper, we develop the necessary theoretical tools for the synthesis of optimizing control structures of chemical plants. In the second part of the paper, implementational problems are addressed; sound and practical strategies or operational policies are systematically derived to implement the optimizing control activities on-line.

CONCLUSIONS AND SIGNIFICANCE

A steady-state design approach has been developed for the synthesis of optimizing control systems of integrated chemical plants, utilizing hierarchical control concepts and the Kuhn-Tucker theory of nonlinear programming for large scale systems. Such a fundamental and modular framework allows the designer: (a) to partition the integrated plant to its subsystems and consequently facilitate the analysis and design procedure; (b) to synthesize practical decentralized optimizing controllers for the individual subsystems; (c) to systematically generate alternative optimizing routes (i.e., a class of set-point changes) which can be implemented on-line by the decentralized subsystem controllers; (d) to analyze the primary interactions among the subsystems and the alternative optimizing routes from an engineering point of view; and (e) to select the best optimizing route for the particular plant.

Finally, an extensive numerical study on a large-scale gasoline polymerization plant demonstrates all the features of this design approach and indicates future research directions on this problem.

FORMAL STATEMENT OF THE PROBLEM

The chemical plant will be first decomposed to its subsystems with functional uniformity and common objectives in terms of economics and operation. Quantitative measures for such decomposition have been established in the Part I of this series by Morari, Arkun and Stephanopoulos (1980a), that attempt to minimize the joint tasks of the subsystems' coordinator and of the local subsystem optimizers.

Steady-State Optimization Problem

Assuming that the plant has been decomposed to N subsystems, we have the following set of equations governing each subsystem S_i at steady-state conditions.

For S_i, $i = 1, \ldots, N$

$$(L_{S_i})\begin{cases} f_i(x_i, m_i, u_i, d_i) = 0 & \text{Subsystem System Equations} \\ r_i(x_i, m_i, u_i, d_i) = r_{i,d} & \text{Subsystem Regulatory Control Task Constraints} \\ y_i = h_i(x_i, m_i, u_i, d_i) & \text{Input-Output Transformation Equations} \\ g_i(x_i, m_i, u_i, d_i) \le b_i & \text{Subsystem Design Constraints} \\ -d_i + d_i^* = 0 & \text{Disturbance Specifications} \end{cases}$$

The vector of inputs u_i results from the interconnections of subsystem i with the other subsystems of the plant and is described by:

$$u_i = \sum_{j=1}^{N} Q_{ij} y_j = Q_i y$$

where y_j is the vector of outputs of subsystem j and Q_i is the incidence matrix describing the interconnections of subsystem i with other subsystems. x_i is the vector of states, m_i is the vector of free manipulated variables, and r_i is the vector of regulatory control constraints which have to be always satisfied (e.g., fixed production rate, product quality specification, etc.). The inequality design constraints reflect certain limitations on process variables which result from safety aspects, equipment capacity and operational requirements. d_i is taken to be the vector of nonstationary, "slow" disturbances with major economic impact on the optimal operation of the plant. d_i^* is the vector of nominal design values of disturbances. For details on the classification of disturbances, the reader should refer to Part I of this series by Morari, Arkun and Stephanopoulos (1980a).

For "slow" disturbances, the plant can be assumed to be at pseudo-steady state, and the following static optimization problem is now considered:

$$
(P_D)\begin{cases} \text{Min}\Phi = \sum_{i=1}^{N} \phi_i(x_i, m_i, u_i, d_i) \\ \text{Subject to the Constraints } (L_{S_i}) \text{ and Interconnection} \\ \text{Constraints} \\ u_i = Q_i y \text{ for } i = 1, \ldots, N. \end{cases}
$$

We assume the overall plant objective function Φ to be the sum of the subsystem objectives Φ_i, i.e., subsystem operating costs. The Lagrange function for (P_D) can now be defined as:

$$L = \sum_{i=1}^{N} l_i(x_i, m_i, u_i, d_i)$$

where the sub-Lagrangian l_i for a subsystem i, $i = 1, 2, \ldots, N$, is given by:

$$l_i = \Phi_i(x_i, m_i, u_i, d_i) - \lambda_i^T u_i + \sum_j \lambda_j^T Q_{ji} y_i.$$

λ_i is the vector of Lagrange multipliers associated with the interconnection constraint $u_i = Q_i y$. From nonlinear optimization theory it is well known that under certain assumptions of convexity the saddle point of the Lagrangian L is the solution to the problem (P_D) (Lasdon, 1970; Wismer, 1971). As a result, L has to be minimized with respect to m_i and u_i and that immediately formulates N first-level subproblems for the subsystems:

Subproblem for S_i, $i = 1, \ldots, N$ (First-Level Problem).

$$\underset{u_i, m_i}{\text{Min}} l_i = \Phi_i - \lambda_i u_i + \sum_j \lambda_j^T Q_{ji} y_i$$

subject to the subsystem constraints (L_{S_i}).

The minimum of l_i depends on the Lagrange multipliers λ_i.

The solutions to the N subproblems will give the solution to the overall problem (P_D) if and only if λ_i's are properly chosen. This formulates the coordinator (the second-level) problem as follows:

Coordinator Problem (Second-Level Problem).

$$\text{Max}\left\{H(\lambda) = \sum_{i=1}^{N} h_i(\lambda)\right\}$$

subject to $\lambda \epsilon D$, where $D = \{\lambda$: the subproblems of the first-level have a solution$\}$.

It also follows that the gradient of the objective function for the second level is the imbalance of the interaction variables, i.e.,

$$\nabla_{\lambda_i} H(\lambda) = \tilde{u}_i - \sum_j Q_{ij} \tilde{y}_j.$$

Therefore, the coordinator attempts to coordinate the subproblem solutions by trying to satisfy the interaction balance:

$$u_i = \sum_{j=1}^{N} Q_{ij} y_j \quad i = 1, \ldots, N$$

while changing λ_i's.

Classification of the Constraints at the Design Optimum

Most of the time the optimal operating point of a well-designed plant is not on a hill-top but lies at the intersection of certain plant constraints (Lee and Weekman, 1976; Rijnsdorp, 1967; Maarleveld and Rijnsdorp, 1970; Baxley, 1969; Kaiser, 1966; Kuehn and Davidson, 1961; Shah, 1970; C. Ishida, 1975; Rijckaert et al., 1978; Kenney, 1979). In mathematical terms, some of subsystem inequality design constraints g_i will become active at the optimum of (P_D) which can be calculated by the two-level optimization method. Therefore, at the design optimum X^* for nominal disturbance values d_i^* $i = 1, \ldots, N$, the inequality constraints of each subsystem S_i can be partitioned as follows:

$$g_i = \begin{bmatrix} g_{i,A}\text{: Active Subsystem Constraints} \\ g_{i,IA}\text{: Inactive Subsystem Constraints} \end{bmatrix}$$

The classification of the inequality constraints constitutes the starting point for the synthesis of decentralized optimizing controllers which we will outline in the following sections.

Selection of the Controlled and Manipulated Variables for the Decentralized Optimizing Controllers

The idea is to design local optimizing controllers for each subsystem S_i of the decomposed plant. Those controllers will be called *decentralized* since each of them will have its local measurements and manipulated variables confined within the boundary of its subsystem. We will select the primary controlled variables c_i^p from the active constraints $g_{i,A}$ and the regulatory control constraints r_i which must be regulated at their current optimum set-points $b_{i,A}$ and $r_{i,d}$, respectively. Thus, the controlled variables can be partitioned as follows:

$$c_i^p(x_i, m_i, u_i, d_i) = [c_{i,reg}^p; c_{i,opt}^p]^T \equiv [r_i; g_{i,A}]^T$$

with desired set-points,

$$c_{i,d}^p = [r_{i,d}; b_{i,A}]^T.$$

Process variables other than "active constraints" could have been selected as the primary controlled variables, but with major drawbacks with respect to the feasibility and robustness of plant operation as demonstrated in Part IV (Arkun and Stephanopoulos, 1980). Primary variables c_i^p will directly identify the measurements within a subsystem S_i. If any of these desired variables cannot be measured, they will be replaced by "secondary" measurements within the particular subsystem. For the optimum selection of "secondary" measurements to estimate the primary variables, the reader should refer to Weber and Brosilow (1972), Joseph and Brosilow (1978), and Part III of the series by Morari and Stephanopoulos (1980c).

Next, manipulated variables m_i for the decentralized controllers have to be selected. The algorithm given in Part II by Morari and Stephanopoulos (1980b) is used to generate all the alternative feasible decentralized control structures where alternative subsets m_{iD} are selected (based on structural controllability-observability concepts) to control c_i^p.

Select m_{iD} in such a way that $m_i = [m_{iD}; \tilde{m}_i]^T$ with $dim(m_{iD}) = dim(c_i^p)$ where $dim(\tilde{m}_i)$ are the remaining degrees of freedom within subsystem i at the design optimum.

Through decomposition and proper formulation of the subsystem control objectives, the selection of the controlled and manipulated variables can be done for individual subsystems in a *decentralized* fashion. Such a decomposition approach will significantly facilitate the overall design strategy and will arrive at decentralized optimizing controllers C_i's each of which has a distinct set of local measurements and manipulated variables within S_i.

Dynamic Evolution of the Steady-State Optimal Plant Operation Policy: Economic Impact of Disturbances

The chemical plants are most of the time subject to persistent economic disturbances such as changing raw materials, product specifications, etc. In order to cope with such a dynamic environment, chemical plant operation has to remain feasible and optimal within a broad operating regime. Current industrial practice dictates that the optimal operating point for a chemical plant will move from the intersection of one set of constraints to another as disturbances change. The importance of constraints in plant economics and operation has been demonstrated on distillation columns (Duyfjes et al., 1973; Rijnsdorp, 1967; Maarleveld and Rijnsdorp, 1970; Kenney, 1979; Roffel and Fontein, 1979), fluid catalytic crackers (Lee and Weekman, 1976; Davis et al., 1974; Webb et al., 1977; Prett and Gillette, 1979) and ethylene plants (Kaiser et al., 1966; Ishida, 1975; Rijckaert et al., 1978; Duncanson and Youle, 1970) with a growing interest to operate chemical plants under "constraint control."

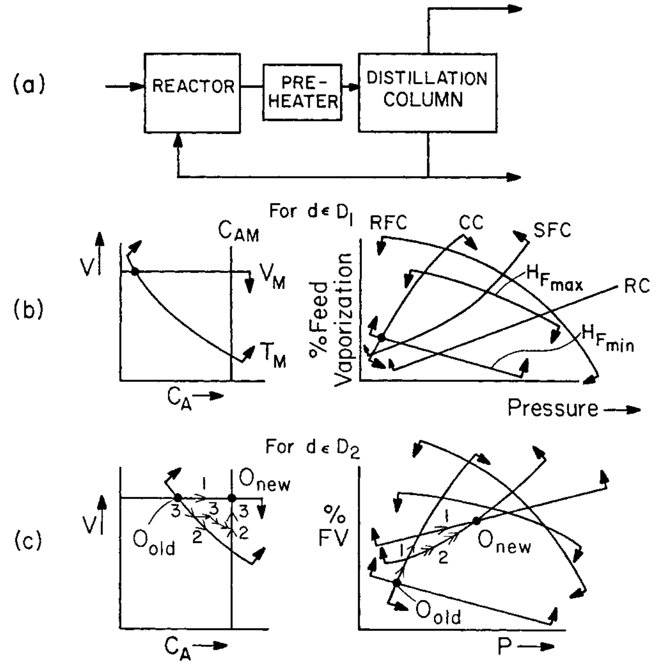

Figure 1. A simple interconnected structure (a), with its subsystems' feasible operational envelopes (b and c).
RFC—Rectifying section flooding constraint
CC —Condensor constraint
SFC—Stripping section flooding constraint
RC —Reboiler constraint
H_F —Feed preheater constraint

As disturbances deviate significantly from their design values d^* to affect the location of the optimum operating point, different options can be considered as alternative optimizing control strategies (Arkun and Stephanopoulos, 1980). In the following sections, we will consider the design of optimizing controllers that will continuously update the optimal plant operation by carrying out the necessary set-point changes. To demonstrate the need for such an optimizing control system, in Figure 1 we give a simple interconnected plant composed of a reactor and a distillation column with a feed preheater. The feasible operating region for the reactor and distillation column subsystems are defined by the design constraints imposed on each unit within these subsystems. For the reactor subsystem the holdup V, temperature T and the exit concentration of the reactant C_A are constrained by the maximum design limits V_m, T_m, C_{Am}. the second subsystem is composed of the distillation tower together with its auxiliary heaters (e.g., reboiler, preheater) and cooler (e.g., condensor) which are the integral parts of the column itself. The subsystem's feasible region is defined by the flooding constraints in different sections of the tower, by the condensor and reboiler constraints due to design and heat transfer limitations and by the constraints on the flowrate of the heating fluid in the preheater (e.g., H_F). As process disturbances such as reactor feed flowrate, temperature, concentration, cooling water temperature or managerial disturbances such as different product specification, production rates, specific heating cost or specific product value, change, different sets of active constraints will determine the optimum. In Figures 1(b) and (c), this dynamic evolution of the steady-state optimum is shown for feed disturbances (flowrate and composition) taking two different sets of values D_1 and D_2. Within each subsystem, the constraints move with disturbances and the local optimum switches from one set of constraints to another. Therefore, the local optimizing controller for each subsystem has to update its optimal operation policy by moving the operation of the subsystem to its new optimum. The important questions to be answered are: how do we select a search strategy (i.e., a sequence of set-point changes) to be implemented on-line by the subsystem optimizing controllers? When do the constraints move and how do we cope with moving constraints? How should the decentralized optimizing controllers be designed to deal with changing active constraints in the presence of disturbances? In the following sections, theoretical developments address all these important problems.

THEORETICAL DEVELOPMENTS

In this section, we will present the theoretical foundations to develop the steady-state optimizing control systems for interconnected systems. Again, we consider that as disturbances with economic impact enter our plant, the optimal operating point changes and calls for optimizing control action. The subsequent analysis will point out how to design the optimizing control structures and establish a search strategy to be employed by the subsystem controllers.

Development of Initial Search Directions (ISD)

Let us consider that the disturbances with serious economic impacts deviate from their design values, i.e., $d_i = d_i' = d_i^* + \delta d_i$, $i = 1, 2, \ldots, N$, and the corresponding optimal operating point switches to the intersection of a different set of constraints. The current design optimum X^* at which the plant has been operating will now constitute the operating point from which the search towards the new optimum will start. As the first step towards the construction of the initial search directions, we need to find *a feasible operating point* for the structured set of equations (L_{S_i}) for $i = 1, \ldots, N$, for the new values of disturbances $d_i = d_i'$. A feasible point algorithm for structured chemical engineering design systems with many constraints as developed by DeBrosse and Westerberg (1973) can be effectively used to locate such a feasible point.

At the new feasible point X^o, some of the previously inactive subsystem constraints will become active, i.e.:

$$g_{i,IA} = \begin{bmatrix} \bar{g}_{i,IA} - \bar{b}_{i,IA} = 0 \\ \tilde{g}_{i,IA} - \tilde{b}_{i,IA} < 0 \end{bmatrix}.$$

Since new active constraints $(\bar{g}_{i,IA})$ are introduced, some of the previously active constraints will now become inactive in order to keep the determinancy feature of the subsystems. Thus, at X^o

$$c^p_{i,opt} = \begin{bmatrix} \bar{c}^p_{i,opt} - \bar{c}^p_{i,d,opt} = 0 \\ \tilde{c}^p_{i,opt} - \tilde{c}^p_{i,d,opt} < 0 \end{bmatrix}$$

Criterion to Select ISD by Local Optimizing Controllers

Once the constraint sets are modified for each subsystem, the initial search direction for each local optimizer C_i of S_i can be selected. Starting at the current optimum X^* where the controlled variables are $c^p_{i,reg}$ (regulatory objectives), $c^p_{i,opt}$ (active inequality constraints), each local optimizing controller C_i will:

(i) *Release* $\tilde{c}^p_{i,opt} \in c^p_{i,opt}$ where $\tilde{c}^p_{i,opt}$: i^{th} subsystem constraints that moved into their feasible region at X^o in response to $d' = d^* + \delta d$.

(ii) Keep $\bar{c}^p_{i,opt} \in c^p_{i,opt}$ *tight* where $\bar{c}^p_{i,opt}$: i^{th} subsystem constraints that are still active at X^o for $d' = d^* + \delta d$.

Each local optimizing controller C_i will know which constraints to release and which ones to hold, moving from X^* to X^o. This will in turn partition the local control loops for each S_i into new classes of regulatory and servo loops in a decentralized fashion.

Partitioning of Subsystem Control Loops.

(1) The controlled variables $\tilde{c}^p_{i,opt}$ (released constraints) will identify the initial *servo loops* for subsystem S_i.

(2) The controlled variables $\bar{c}^p_{i,opt}$ (tight constraints) together with $c^p_{i,reg}$ will define the *regulatory loops* for subsystem S_i.

Initial Search Towards X^o. Each local controller C_i with a partitioned set of controllers will change set-points $\tilde{c}^p_{i,d,opt}$ of its *servo loops* while regulating $\bar{c}^p_{i,opt}$ and $c^p_{i,reg}$ at their fixed set-points $b_{i,A}$ and $r_{i,d}$, respectively.

Updating Control Structure at Feasible Point X^o. After the feasible point is attained, we redefine at X^o the primary control variables for each susbystem S_i:

$$c_i^p = \begin{bmatrix} c_{i,reg}^p(x_i, m_{iD}, \tilde{m}_i, u_i, d_i') \\ \bar{c}_{i,opt}^p(x_i, m_{iD}, \tilde{m}_i, u_i, d_i') \\ \bar{g}_{i,IA}(x_i, m_{iD}, \tilde{m}_i, u_i, d_i') \end{bmatrix} \equiv \begin{bmatrix} c_{i,reg}^p \\ c_{i,opt}^p \end{bmatrix}$$

Regulatory control task variables $c_{i,reg}^p$ are carried along from one operating point (X^*) to another (X^o) whereas controlled variables resulting from optimizing control task (i.e., $c_{i,opt}^p$) change as new constraints (i.e., control objectives) are encountered. Since the previously active constraints $\bar{c}_{i,opt}^p$ are inactive at X^o, they are no longer our control objectives. The manipulated variables which have been engaged in the control of $\bar{c}_{i,opt}^p$ together with any other free manipulated variable $\tilde{m}_i$ can now be used to control the new constraints $\bar{g}_{i,IA}$. Any resulting alternative control structure where c_i^p will be controlled by alternative sets of m_{iD} (where $dim\ c_i^p = dim\ m_{iD}$) will have to be feasible in terms of structural controllability and observability. The feasibility check can be performed on individual subsystem controllers using the algorithm developed in Part II of the series (Morari and Stephanopoulos, 1980b).

New Search Direction (NSD) Selection at X^o. After each subsystem achieves feasible operation via its initial search direction, the second phase of the optimizing control actions will consist of determining and following new search directions towards the new optimum.

Lagrangian Formulation. After the set of active and inactive constraints are modified and the controlled and manipulated variables are identified for each subsystem at X^o, the initial subsystem equations (L_{S_i}) will become:

For S_i, $i = 1, \ldots, N$

$$(L_{D_i}) \quad \begin{cases} f_i(x_i, m_{iD}, \tilde{m}_i, u_i, d_i) = 0 \\ c_{i,reg}^p(x_i, m_{iD}, \tilde{m}_i, u_i, d_i) - c_{i,d,reg}^p = 0 \\ c_{i,opt}^p(x_i, m_{iD}, \tilde{m}_i, u_i, d_i) - c_{i,d,opt}^p = 0 & \text{New Active Constraints} \\ g_{i,IA}(x_i, m_{iD}, \tilde{m}_i, u_i, d_i) < b_{i,IA} & \text{New Inactive Constraints} \\ y_i = h_i(x_i, m_{iD}, \tilde{m}_i, u_i, d_i) \\ -d_i + d_i' = 0 \end{cases}$$

where the set-points are:

$$c_{i,d,reg}^p = r_{i,d}$$
$$c_{i,d,opt}^p = b_{i,A}$$

The Lagrange function for the decomposed optimization problem P_D can now be reformulated as follows:

$$L = \sum_{i=1}^{N} l_i(\tilde{m}_i, u_i, c_{i,d,reg}^p, c_{i,d,opt}^p, d_i)$$

in terms of the sub-Lagrangians l_i, with

$$l_i = \Phi_i(\tilde{m}_i, u_i, c_{i,d,reg}^p, c_{i,d,opt}^p, d_i) - \lambda_i^T u_i + \sum_j \lambda_j^T Q_{ji} y_i - \Pi_i^T(d_i - d_i')$$

where x_i and m_{iD} are not present since they are uniquely determined for given set-points $c_{i,d,reg}^p$ and $c_{i,d,opt}^p$ and inputs $\tilde{m}_i$, u_i, d_i through the subsystem constraints (L_{D_i}).

Substituting $y_i = h_i(\tilde{m}_i, u_i, c_{i,d,reg}^p, c_{i,d,opt}^p, d_i)$ and expanding L to first-order terms gives:

$$\delta L = \left[\frac{\partial \Phi_i}{(\partial c_{i,d,opt}^p)^T} + \sum_j \lambda_j^T Q_{ji} \frac{\partial h_i}{(\partial c_{i,d,opt}^p)^T}\right]\delta c_{i,d,opt}^p + \left[\frac{\partial \Phi_i}{\partial u_i^T} - \lambda_i^T + \sum_j \lambda_j^T Q_{ji} \frac{\partial h_i}{\partial u_i^T}\right]\delta u_i + \left[\frac{\partial \Phi_i}{\partial \tilde{m}_i^T} + \sum_j \lambda_j^T Q_{ji} \frac{\partial h_i}{\partial \tilde{m}_i^T}\right]\delta \tilde{m}_i$$

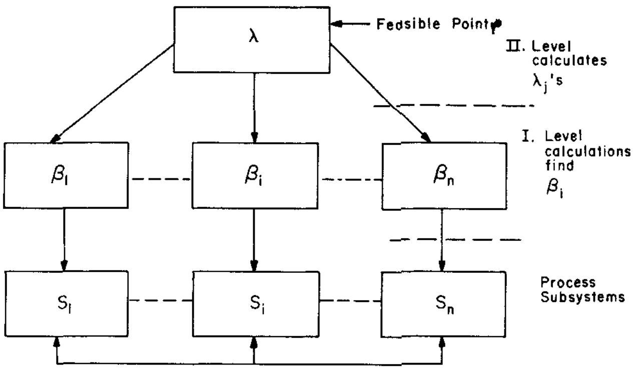

Figure 2. Computational hierarchy to evaluate Kuhn-Tucker multipliers (KTM) and find new search directions (NSD).

+ Other Terms in δd_i, δu_i, $\delta c_{i,d,opt}^p$, $\delta \tilde{m}_i$, $\delta \Pi_i$, $\delta \lambda_i$ for All Subsystems.

In order for the current operating point X^o to be optimum, the following necessary stationarity conditions for the minimum of $\Phi = \Sigma \Phi_i$ should hold at X^o:

For $i = 1, \ldots, N$

$$\nabla_{\tilde{m}_i} L = \left(\frac{\partial \Phi_i}{\partial \tilde{m}_i} + \sum_j \frac{\partial h_i^T}{\partial \tilde{m}_i} Q_{ji} \lambda_j\right) = 0 \quad \text{Constrained Derivatives}$$

$$\nabla_{u_i} L = \left(\frac{\partial \Phi_i}{\partial u_i} - \lambda_i + \sum_j \frac{\partial h_i^T}{\partial u_i} Q_{ji} \lambda_j\right) = 0 \quad \text{Adjoint Equations}$$

$$\nabla_{d_i} L = \frac{\partial \Phi_i}{\partial d_i} - \Pi_i + \sum_j \frac{\partial h_i^T}{\partial d_i} Q_{ji} \lambda_j = 0$$

$$u_i - \sum_j Q_{ij} y_j = 0$$

$$d_i - d_i' = 0$$

$$g_{i,IA} < b_{i,IA}.$$

and the Kuhn-Tucker conditions are:

(i) $\beta_i < 0$

(ii) $\beta_i^T(c_{i,opt}^p - c_{i,d,opt}^p) = 0$

where β_i is the vector of Kuhn-Tucker multipliers associated with the i^{th} subsystem active constraints, and it is given by

$$\beta_i = \frac{\partial \Phi_i}{\partial c_{i,d,opt}^p} + \sum_j \frac{\partial h_i^T}{\partial c_{i,d,opt}^p} Q_{ji} \lambda_j. \tag{1}$$

Criterion to Select NSD

The sign of the Kuhn-Tucker multipliers (KTM) will show us how the plant objective function Φ will change with a movement to the interior of the feasible region of an active constraint. For example, $\beta_{i,j} < 0$ shows that an infinitesimal move to the interior of $c_{j,opt}^p$, holding other constraints tight, will increase Φ; therefore, $c_{j,opt}^p$ should be held tight.

In order for the i^{th} subsystem controller to evaluate its β_i, it needs to know λ_j's, the prices of its outputs at the current point. The adjoint set of equations, $\nabla_{u_i} L = 0$ $i = 1, \ldots, N$, can be easily solved (Westerberg, 1973) to find these prices. In a summary, the computational decomposition is shown in Figure 2. After KTM's are calculated, new search directions within the i^{th} subsystem can be found as follows:

(1) If $\beta_{i,j} < 0$, keep $c_{j,opt}^p$ tight

(2) If $\beta_{i,j} > 0$, release $c_{j,opt}^p$

Repartitioning of Subsystem Control Loops

The current control loops of each subsystem's optimizing controller C_i will be partitioned into *servo* and *regulatory* loops according to the new search direction selected:

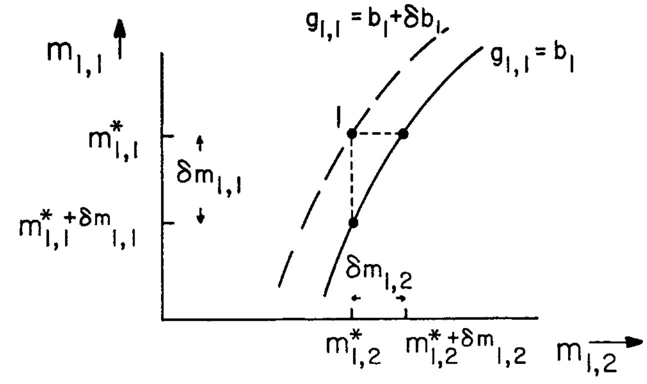

Figure 3. Study of constraint movement. – – – – location of the constraint before disturbance changes. ——— location of the constraint after disturbance changes.

(1) Released set of constraints (i.e., $\beta_{ij} > 0$) $c^p_{i,R}$ will identify the *servo loops*.

(2) Tight constraints $c^p_{i,T}$ and $c^p_{i,reg}$ will define the *regulatory* loops.

Current Control Loops at X^o: $[c^p_i] \nearrow [c^p_{i,opt}] \nearrow [c^p_{i,R}]$: New Servo Loops; $[c^p_{i,opt}] \searrow$, $[c^p_i] \searrow [c^p_{i,reg}] \mapsto \begin{bmatrix} c^p_{i,T} \\ c^p_{i,reg} \end{bmatrix}$: New Regulatory Loops

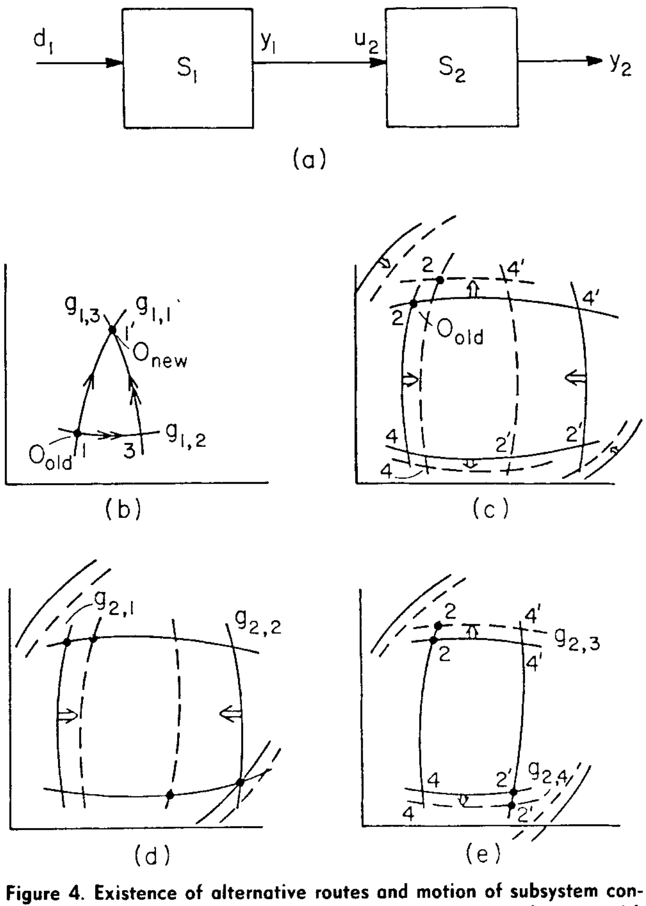

Figure 4. Existence of alternative routes and motion of subsystem constraints in response to different set-point changes in a serial system with noninteracting subtrees. (a) A simple serial system. (b) Alternative routes for subsystem S_1. (c) Movement of the constraints of S_2 in response to set-point changes along the route 1 → 1′ for subsystem S_1. (d) Movement of the constraints of S_2 in response to set-point changes along the route 1 → 3 for subsystem S_1. (e) Movement of the constraints of S_2 in response to set-point changes along the route 3 → 1′ for subsystem S_1.

Search Process towards New Optimum

The original steady-state optimization problem for the decomposed plant can now be formulated as:

$$\text{Min}\Phi = \sum_{i=1}^{N} \Phi_i(c^p_{i,R,d},\ c^p_{i,T,d},\ c^p_{i,d,reg},\ \tilde{m}_i)$$

(P'_D)

subject to

$$g_{i,IA}(c^p_{i,R,d},\ c^p_{i,T,d},\ c^p_{i,d,reg},\ \tilde{m}_i) - b_{i,IA} \le 0 \quad i = 1, \ldots, N.$$

At each optimization step, local optimizing controllers change the set-points of the released constraints $c^p_{i,R,d}$ and $\tilde{m}_i$ (if available), and the system constraints (L_{Di}), $i = 1, \ldots, N$ are always satisfied to give the values of the dependent variables x_i, m_{iD}, $g_{i,IA}$ and of the subsystem objectives Φ_i's. As a result, the search algorithm towards the optimum consists of a sequence of plant feasible operating points where the structured design equations (L_{Di}) are continuously modified and solved during optimization.

Search Interruption

When subsystems modify the set-points $c^p_{i,R,d}$ and $\tilde{m}_i$ (if available), some of the inactive constraints $g_{i,IA}$ will become active. The following control structure modification will then be performed locally for C_i to accommodate the new control objectives (Arkun, 1979):

(i) New active constraints $\bar{g}_{i,IA} \epsilon g_{i,IA}$ in S_i will be controlled at set-points $\bar{b}_{IA}$.

(ii) $dim(\bar{g}_{i,IA})$ controlled variables $\bar{c}^p_R$ which have moved into their feasible region will be deleted from the set of released constraints $c^p_{i,R}$ and will not be controlled any more.

Hence, the new set of regulatory and servo loops for S_i becomes:

$[c^p_{i,T};\ \bar{g}_{i,IA}]$: New Regulatory Loops

$[\bar{c}^p_{i,R}]$: New Servo Loops

with the following modified set of inactive constraints

$$g_{i,IA} = [\bar{c}^p_{i,R};\ \tilde{g}_{i,IA}]^T.$$

The search will be continued by changing set-points of the new servo loops and whenever new constraints are encountered, control structure changes will be done locally in that subsystem, in a decentralized fashion. If the Kuhn-Tucker multipliers associated with the tight constraints in all subsystems are all negative, an apparent minimum is found and the search is terminated.

IMPLEMENTATIONAL STRATEGIES FOR INTERCONNECTED SYSTEMS

The theoretical developments of the previous section lead to a constrained steady-state optimization problem which is solved within the framework of hierarchical control using the Kuhn-Tucker theory of nonlinear programming. The solution algorithm generates alternative practical control strategies that can be implemented on-line by the subsystems' decentralized optimizing controllers, as a sequence of set-point changes (i.e., optimization steps).

The aim of the present section is to explore the implementational problems for the optimizing control of interconnected systems. The formulation and the significance of these problems for chemical plants will be laid down first, before attempting to structure any practical strategy for such complex systems. The design approach that will be formulated will deal with those features common to all interconnected systems, and thus it will have the broad applicability to any interconnected system. The steps to be taken during the design stage will be general although the implementational problems will vary in complexity from one system to another.

Sequencing Problem for Interconnected Systems

Each subsystem of the decomposed plant will have its own economic subobjective and feasible operating region like the one shown in Figure 1(b). The following important features should be emphasized:

(i) By a first-order perturbation analysis, it will be later shown that the subsystem constraints move with changes in external disturbances, d_i. This produces different boundaries of the feasible regions and different points of optimum operation for the individual subsystems (see Figure 1(c)).

(ii) As delineated by the theoretical developments, to move from one optimum to another, alternative operational routes, each describing different control strategies (i.e., different regulatory feedback structures and *sequence* of set-point c' anges), will exist for each subsystem's optimizing controller, Figure 1(c).

(iii) As we will formulate in the next section, the subsystem constraints move and the feasible region boundary changes in response to different interconnection inputs, u_i. In the reactor-distillation example, as the set-points of the reactor servo control loops are changed, the feasible region of the distillation subsystem will change in response to the new values of its input from the reactor. Similarly, the feasible region of the reactor will also change due to the recycle input from the distillation unit. This dynamic evolution of the feasible regions due to the interaction of interconnected subsystems brings out important questions to be answered during the development of the sequencing strategy (i.e., optimization routes as described by a sequence of set-point changes) for a complete chemical plant.

For given values of external disturbances and interconnection inputs, the feasible region and the alternative routes (*a sequencing subtree*) can be generated *for each subsystem* separately (Arkun and Stephanopoulos, 1980). The central design question is how to generate the sequencing tree for the integrated plant from such subtrees. Once the sequencing tree for the plant is developed, screening strategies will have to be devised to select the best sequence to be implemented. In order to analyze these problems and demonstrate the associated design activities, we proceed with the mathematical analysis of the dynamic evolution of the subsystems' feasible regions.

Motion of Constraints: a Mathematical Formulation (Arkun, 1979)

The motion of constraints for different subsystems can be demonstrated by a linear perturbation analysis. For a plant with N subsystems, assume the following nonlinear model is valid for each subsystem S_i at steady-state,

$$f_i(x_i, m_i, u_i, d_i) = 0$$
$$g_i(x_i, m_i, u_i, d_i) \leq b_i$$
$$y_i = h_i(x_i, m_i, u_i, d_i)$$

where some of the variables are reclassified so that m_i is the vector of variables representing the coordinates of the feasible region (e.g., in Figure 1(b), $m_1 = [VC_A]^T$, $m_2 = [\%FV\,P]^T$). x_i is the vector of dependent variables and u_i, d_i, y_i are as defined before.

The movement of constraints g_i in the space spanned by m_i is governed by the following equation,

$$\delta m_{i,j} = \frac{\left[\frac{\partial g_{i,k}}{\partial d_i^T} - \frac{\partial g_{i,k}}{\partial x_i^T} J_i^{-1} D_i\right]\delta d_i}{\left[\frac{\partial g_{i,k}}{\partial m_{i,j}} - \frac{\partial g_{i,k}}{\partial x_i^T} J_i^{-1} M_i I_j\right]} + \frac{\left[\frac{\partial g_{i,k}}{\partial u_i^T} - \frac{\partial g_{i,k}}{\partial x_i^T} J_i^{-1} U_i\right]\delta u_i}{\left[\frac{\partial g_{i,k}}{\partial m_{i,j}} - \frac{\partial g_{i,k}}{\partial x_i^T} J_i^{-1} M_i I_j\right]}$$

$$\equiv \gamma_{d_i}^T \delta d_i + \gamma_{u_i}^T \delta u_i \quad (2)$$

where the constant matrices are defined by:

$$J_i = \left[\frac{\partial f_i}{\partial x_i^T}\right], \quad D_i = \left[\frac{\partial f_i}{\partial d_i^T}\right],$$

$$M_i = \left[\frac{\partial f_i}{\partial m_i^T}\right], \quad U_i = \left[\frac{\partial f_i}{\partial u_i^T}\right], \quad I_j = \begin{bmatrix} 0 \\ 0 \\ \vdots \\ 1_j \\ 0 \\ \vdots \\ 0 \end{bmatrix} \text{ And Are Evaluated}$$

at the steady-state operating point.

The value of $\delta m_{i,j}$ shows how far the k-th inequality design constraint $g_{i,k}$ in subsystem i travels along the direction of the j^{th} coordinate $m_{i,j}$, in response to: (a) disturbances d_i entering S_i; (b) interconnection inputs u_i from the other subsystems. Some constraints will move very little and some will shift considerably depending on the magnitudes of the steady-state gains γ_{d_i}, γ_{u_i}. In Figure 3, the movement of a single constraint in a two-dimensional feasible region is illustrated.

The second term of Eq. 2 reflects how the subsystem feasible regions are coupled with each other through the interconnections. We will call this *the interaction term* and analyze how it is related to the optimizing control actions of the decentralized subsystem controllers. As derived in Appendix, linear perturbations for the decomposed plant yield,

$$\delta u = A^{-1}[B\delta c_d^p + C\delta\tilde{m} + K\delta d] \quad (3)$$

where

$$\delta u = \begin{bmatrix} \delta u_1 \\ \vdots \\ \delta u_i \\ \vdots \\ \delta u_N \end{bmatrix}; \quad \delta c_d^p = \begin{bmatrix} \delta c_{1,d}^p \\ \vdots \\ \delta c_{i,d}^p \\ \vdots \\ \delta c_{N,d}^p \end{bmatrix}; \quad \delta d = \begin{bmatrix} \delta d_1 \\ \vdots \\ \delta d_i \\ \vdots \\ \delta d_N \end{bmatrix}; \quad \delta\tilde{m} = \begin{bmatrix} \delta\tilde{m}_1 \\ \vdots \\ \delta m_i \\ \vdots \\ \delta\tilde{m}_N \end{bmatrix}$$

This equation shows that the interconnection input u_i to subsystem i will change when the optimizing controllers of the other interconnected subsystems vary their set-points (i.e., $\delta c_{j,d}^p$), their free manipulated variables (i.e., $\delta\tilde{m}_j$) and when the disturbances enter the subsystems (i.e., δd_j). Hence, Eqs. 2 and 3 together give physical insight and show qualitatively the evolution of the coupled subsystem feasible regions when disturbances enter a chemical plant and when different optimizing control decisions are exercised on-line by different local controllers.

Development of the Plant Control Sequencing Tree

The extent of the design activities involved will depend on how strongly the subsystems' feasible regions are coupled with each other through the interconnections. Two cases will be distinguished as we will examine in the following paragraphs.

(i) *Noninteracting Subtrees.* In this case, the boundary of the subsystem feasible regions will be defined by the same constraints regardless of the value of the interconnection inputs. The fortunate result of such systems is that the subsystem subtrees of alternative optimization routes can be generated independently, and the overall plant sequencing tree can be easily constructed from these noninteracting subtrees. To demonstrate the basic ideas, let us consider a simple serial system of Figure 4(a). To construct the feasible region for S_1, we need to specify the disturbance values d_1. For the feasible region of S_2, we need to know its interconnection input u_2. Since $u_2 = y_1$, the operating point of S_1 will uniquely determine y_1 and thus, u_2.

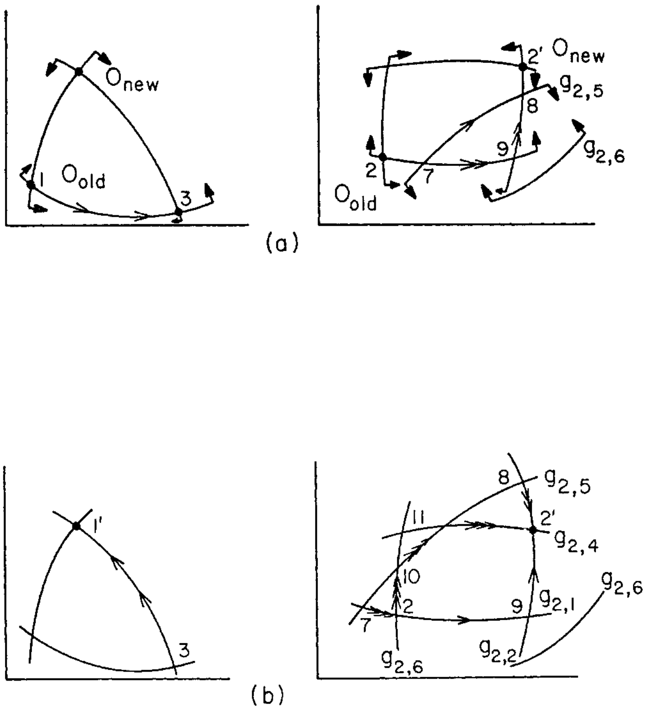

Figure 5. Alternative routes for the second subsystem S_2 when the first subsystem S_1 moves along different constraints in a serial plant with interacting subtrees.

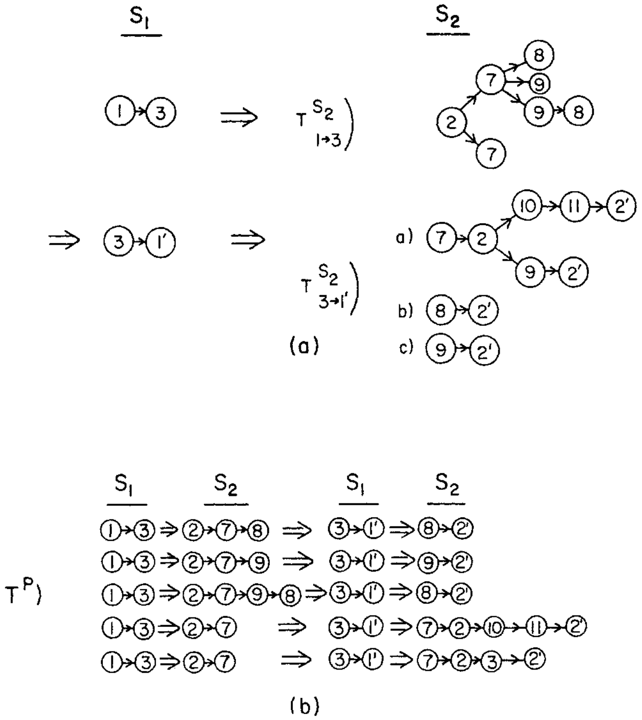

Figure 6. The subtrees (a) and the sequencing alternatives (b) for a simple serial plant.

Let us assume that the feasible regions have been built for the new value of d_1 after it has deviated from its design value and when both subsystems continue to operate at their old design optimum, O_{old}, as shown in Figure 4(b) and (c).

Each decentralized optimizing controller will try to move its subsystem operation from its old optimum to its new optimum (i.e., from 1 to 1′ for S_1; from 2 to 2′ for S_2) by implementing the necessary set-point changes. As illustrated by Figure 4(b), we will have the following subtree, T^{S_1}, of alternative routes for S_1:

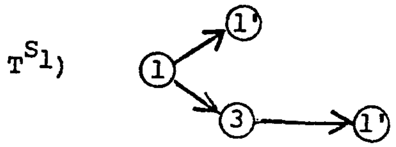

For each intermediate steady state operating point along a route in S_1, u_2 will assume a new value as given by Eq. 3 and determine the motion of constraints in S_2 according to Eq. 2. For

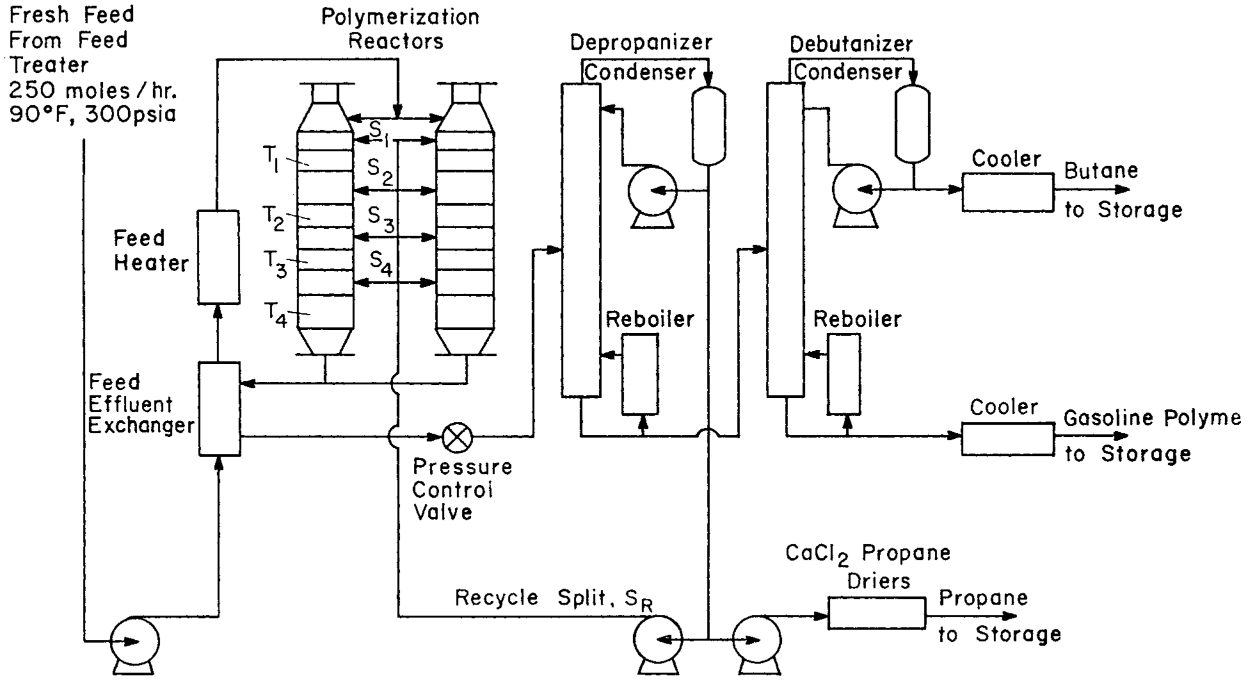

Figure 7. Flow diagram of the gasoline polymerization plant.

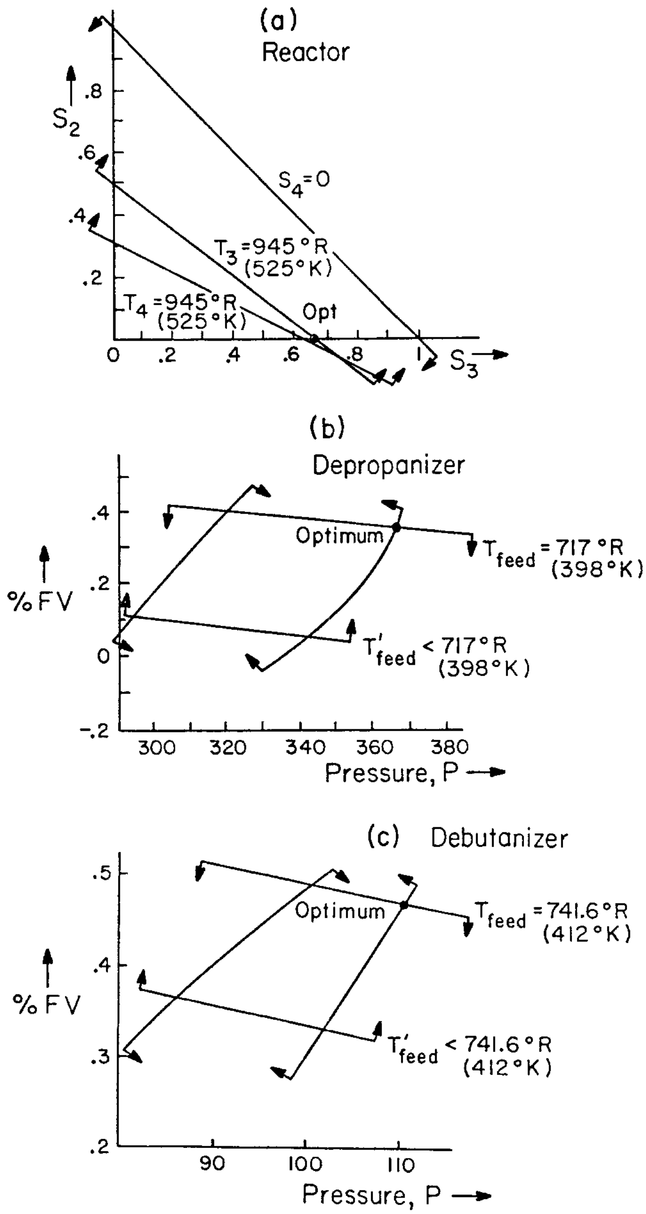

Figure 8. Feasible operating regions for the reactors (a), depropanizer (b), and debutanizer (c) subsystems at the optimal design conditions.

example, along $1 - 1'$, the set-point of $g_{1,2}$ is changed (i.e., $\delta c^p_{1,d} = \delta g_{1,2}$) while $g_{1,1}$ is kept tight, and as a result of this optimizing action the constraints in S_2 move as shown by arrows in Figure 4(c). On the other hand, the constraints in S_2 might behave differently if S_1 moves along the alternative route $1 \rightarrow\!\!\rightarrow 3 \rightarrow\!\!\rightarrow 1'$. Figure 4(d) and 4(e) illustrate the response of constraints when S_1 moves along the two branches $1 \rightarrow\!\!\rightarrow 3$, $3 \rightarrow\!\!\rightarrow 1'$ of this route.

No matter which alternative route is chosen for S_1, the subtree of alternative routes for S_2 will remain the same since the constraint boundary of the feasible region of S_2 is not affected by the set-point changes in S_1. Therefore, the subtree of alternative routes for S_2 is given by:

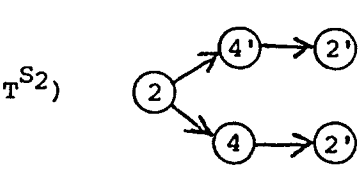

After matching alternative branches of the two subtrees T^{S_1} and T^{S_2}, the following four sequencing alternatives for the overall plant will result:

Total Plant Operation Routes:

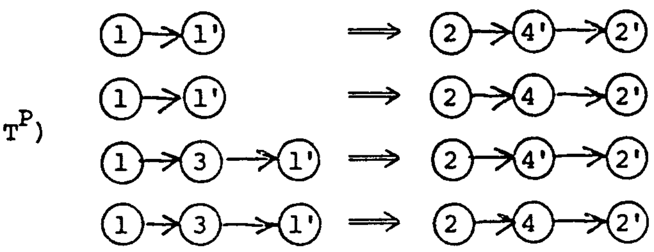

Therefore, for this example, subsystem trees T^{S_1} and T^{S_2} can be designed independently, and the plant tree T^P can then be easily constructed from these subtrees.

(ii) *Interacting Subtrees.* For this class of systems, the constraints which define the boundaries of subsystem feasible regions will change as the interconnection inputs take different values. Let us again consider the serial system of Figure 4(a); but this time S_2 will have different characteristics, i.e., constraint $g_{2,5}$ is assumed to be sensitive to the interconnection input, u_2. For example when S_1 moves to point 3, the feasible region of S_2 might change as shown in Figure 5(a). The constraint $g_{2,5}$ moves more than the others, and the initial design optimum 2 and the new optimum 2′ both become infeasible. When S_1 is at 3, the following subtree will be valid for S_2:

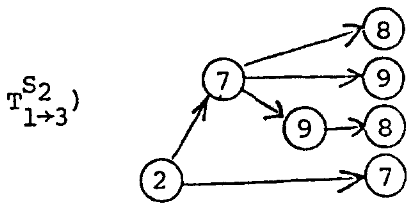

The closest one can get to the optimum is the point 8 beyond which there cannot be any branching without violating the constraint $g_{2,5}$. As S_1 moves from 3 to its optimum 1′, $g_{2,5}$ will move up and $g_{2,6}$ will move down to give the final feasible region as shown in Figure 5(b). When S_1 is at point 1′, the locations of the previous set of alternative final nodes ⑦, ⑧, ⑨ of $T^{S_2}_{1\to3}$ will be determined by the intersection of the corresponding constraints after they have moved. Figure 5(b) indicates that ⑦ and ⑧ will move out of the feasible region with the fast constraint $g_{2,5}$ whereas ⑨ still remains feasible. Now alternative subtrees for S_2 will have to be generated from these nodes ⑦, ⑧, ⑨, towards the optimum, 2′. Thus,

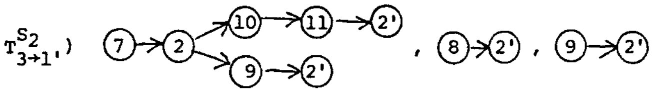

As a result, the sequencing tree T^P for the overall plant, Figure 6(b), will have to be generated from the sequence of subtrees shown in Figure 6(a).

The sequencing starts in S_1 by the route $1 \rightarrow 3$. After S_1 reaches point 3, the subtree of S_2, $T^{S_2}_{1\to3}$ will have four alternative routes which will end at the nodes ⑦ or ⑧ or ⑨. After S_1 reaches its optimum by the route $3 \rightarrow 1'$, the sequencing will restart in S_2 from one of these three nodes. This generates a family of subtrees $T^{S_2}_{3\to1'}$ a), b), c). When a route is selected in $T^{S_2}_{1\to3}$, the subtree to be picked from this family is uniquely determined.

The final node of the route in $T^{S_2}_{1\to3}$ has to match with the initial node of a subtree in $T^{S_2}_{3\to1'}$. Following this rule, the second class of sequencing alternatives for the plant are given in Figure 6(b). Similarly, a different plant tree can be generated if S_1 follows the route $1 \rightarrow 1'$.

Such a design approach to create alternative operational strategies can be applied to any interconnected plant with serial and cyclic structure as demonstrated in detail in the work of

Arkun (1979). The general design approach can be summarized to have the following steps:

(a) Study the impact of a branch followed by one subsystem on the feasible region boundary of all the interconnected systems.
(b) Generate the subsystems subtrees.
(c) Construct the plant sequencing tree from the subtrees.

Screening of Alternative Routes

In this section we will give guidelines to screen among alternative routes of a plant sequencing tree to arrive at an acceptable sequence of set-point changes.

(i) *Screening of Subtrees.* The screening starts with the subtrees of the subsystem where the search is initiated. The branch and bound screening strategy by Arkun and Stephanopoulos (1980) and Arkun (1979) is utilized to screen among the alternative branches of a subtree.

(1) The feasibility of the control structures at the nodes of the subtree are checked and infeasible nodes are closed.
(2) If there exists no control structure with satisfactory steady-state and dynamic characteristics at a particular node, subsystem routes passing through that node will be also rejected.

These screening rules will not only eliminate certain routes within the subtree but will also automatically screen some of the alternative subtrees of the following subsystems. For example, for the serial system of the previous section we have the following subtree for S_1:

T^{S_1})

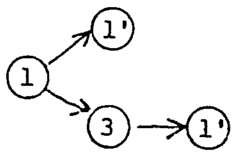

If the branch $1 \rightarrow 3$ is screened and rejected, the subtree $T^{S_2}_{1\rightarrow3}$ in the sequencing tree T^p for the plant will not be acceptable.

After the screening of the first subtree is completed, for each remaining route in S_1 the corresponding second subtree in the sequence is screened. For example, if $1 \rightarrow 3 \rightarrow 1'$ is acceptable in S_1; then the next subtree in the sequence to be screened is:

$T^{S_2}_{1\rightarrow3}$)

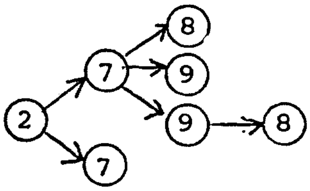

The screening continues until all the subtrees in the sequence are evaluated. In our example, the last subtree is $T^{S_2}_{3\rightarrow1}$.

(ii) *Screening of the Plant Tree.* After screening the subtrees, we obtain a reduced set of alternative routes for the plant. We next find the best sequence of set-point changes among these based upon the following additional factors.

(1) *Plant Safety.* As a first priority any optimizing control action exercised during normal plant operation should not force the plant to a hazardous situation which will lead to disaster. We will propose to make use of adaptive safety interlock system developed by Rivas and Rudd (1974) to analyze and screen the unsafe routes (Arkun, 1979).

(2) *Plant Bottlenecking.* Each alternative plant route will be examined if there is a bottleneck, i.e., if an equipment is required to operate beyond its maximum capacity. Any path leading to such bottlenecks will be rejected.

For the remaining alternatives which are safe and free of bottlenecks, further screening rules similar to those given in Part IV (Arkun and Stephanopoulos, 1980) and Arkun (1979) will be used to select the best route. Those routes which require a large number of set-point changes will not be acceptable. Set-point changes along a route should be smooth and fast enough. The routes with branches along which the plant objective function deteriorates will not be acceptable unless these are the only alternatives. Finally, those routes with minimum number of control structure modifications will be preferred for implementational easiness.

NUMERICAL EXAMPLE

Steady-State Optimizing Control of a Gasoline Polymerization Plant

We will now show how steady-state optimizing control structures can be developed for a large scale chemical plant. We will consider the gasoline polymerization plant shown in Figure 7. This plant has been the object of simulation and optimization studies (Gaines and Gaddy, 1976), and of modeling and process operation optimization (Friedman and Pinder, 1972). The process is the Universal Oil Products solid phosphoric acid catalyst process that produces gasoline from light hydrocarbons. We have studied the plant in Part I (Morari, Arkun and Stephanopoulos, 1980a) in conjunction with the hierarchical decomposition aspects. Three distinct interconnected subsystems with well-defined operational and economic objectives have been found. These are the reactors, the depropanizer, and the debutanizer respectively. We will analyze the effects of important economic disturbances on the optimal performance of the plant, and consequently optimizing control strategies will be generated for the three plant subsystems. The major disturbances to be considered are the feed flowrate, feed composition and the propane recovery in the depropanizer which were found to belong to the optimizing control task. [See Part I (Morari, Arkun, Stephanopoulos, 1980a) for details.] For the simulation of the plant, the simulator CHESS (Motard et al., 1968) and PROPS (Gaines and Gaddy, 1974) were utilized.

Construction of the Feasible Operating Regions for the Subsystems

For the reactor subsystem, the most critical process variables are the four bed temperatures. They are constrained by upper and lower limits to prevent the formation of stable liquid esters and heavy hydrocarbons which would deteriorate the activity of the catalyst. Reactor bed temperature (T_i) constraints together with the physical flow limitations on the depropanizer, the recycle split s_r and the four bed quench splits, s_i, define the inequality design constraints for the reactor subsystem, S_1:

$$g_1 = \begin{bmatrix} 760°\text{R } (422°\text{K}) \le T_i \le 945°\text{R } (525°\text{K}) \\ 0 \le S_r \le 1 \quad i = 1, 2, 3, 4 \\ 0 \le S_i \le 1 \end{bmatrix}.$$

For the depropanizer and debutanizer subsystems, S_2 and S_3, we have the flooding constraints, reboiler constraints and condensor constraints which define the subsystem constraints g_j, $j = 2, 3$:

$$g_j = \begin{bmatrix} \text{Percent Flooding} \le 95\% \\ T_{stm,reb} \le 903°\text{R } (502°\text{K}) \\ \Delta T_{cw} \ge 25°\text{F } (14°\text{C}) \end{bmatrix}$$

where the maximum reboiler steam temperature ($T_{stm,reb}$) available is 903°R (502°K) and minimum increase in the condensor cooling water temperature (ΔT_{cw}) is taken as 25°F (14°C).

Optimal steady-state design conditions for the polymerization plant are given in Table 1. At these optimal design conditions, the feasible region for the reactor subsystem is shown in Figure 8(a). The two quench splits s_2 and s_3 were taken as the free variables to change, and the temperature constraints could then be easily plotted. T_1 and T_2 constraints are not shown in the feasible region since they never become active. For the design conditions, the reactor optimum lies at the intersection of two constraints $s_2 = 0$ and $T_3 = 945°\text{R}$ (525°K) as shown in Figure 8(a). At this point all the remaining reactor operating variables

TABLE 1. OPTIMAL STEADY-STATE DESIGN CONDITIONS FOR THE POLYMERIZATION PLANT

Feed		
Temperature	— 550°R (305.5°K)	
Pressure, psia	— 330 (2.275×10^6 Pa)	
Composition	—	
Propane	—	57.45 mol/h
I-Butane	—	50.00 mol/h
N-Butane	—	45.00 mol/h
I-Pentane	—	7.5 mol/h
N-Butane	—	2.5 mol/h
Propylene	—	42.55 mol/h
Cis-2-Butene	—	10 mol/h
Trans-2-Butene	—	7.5 mol/h
I-Butene	—	25 mol/h
Tr-2-Pentene	—	2.5 mol/h
TOTAL	—	250 mol/h

recycle split $s_r = 0.4647$
quench splits
$s_1 = 0$
$s_2 = 0$
$s_3 = 0.6525$
$s_4 = 0.3475$
depropanizer pressure = 363 psia (2.503×10^6 Pa)
debutanizer pressure = 110 psia (0.758×10^6 Pa)
reactor bed temperatures
T_1 = 815°R (452.8°K)
T_2 = 925°R (513.0°K)
T_3 = 945°R (525°K)
T_4 = 944.9°R (524.95°K)

are uniquely determined and assume the values given in Table 1.

In order to plot the feasible region of the depropanizer, Figure 8(b), the percent feed vaporization and the pressure were taken as the free variables. At the optimum, stripping section flooding constraint was found to be active.

Debutanizer operates at its reboiler constraint as shown in Figure 8(c). Flooding constraints are not plotted since they fall way outside the feasible region of interest.

Selection of the Controlled and Manipulated Variables for Each Subsystem S at the Design Optimum

We will now select the controlled and manipulated variables for each subsystem to construct the decentralized optimizing controllers. At the design optimum, the primary controlled variable for S_1 is the active temperature constraint T_3 of the output stream from the third reactor bed. We will regulate T_3 at its optimal design value 945° by manipulating the quench flow to the third bed, i.e., s_3.

Since the depropanizer optimum is at maximum allowable column capacity, the primary controlled variable is then the tray loads or the pressure drop ΔP_s across the stripping section trays. The most effective manipulated variables to control ΔP_s will be the cooling water flowrate or the heat input to the reboiler. Hence, in addition to the existing column regulatory loops, we have one additional control loop for optimizing control purposes.

Lastly, since debutanizer optimal operation is limited by the reboiler constraint, the steam pressure will be kept at its highest available level which will determine the optimum column pressure.

Analysis of the Effects of Disturbances on the Optimal Plant Performance

We will now turn our attention to the important disturbances and study their impacts on our optimizing control policy. We start with the feed composition disturbances.

A. *The Effect of Propane to Propylene Ratio in the Feed.* The propane to propylene ratio was changed from its design value 1.35 to the new value 1.22 (i.e., the feed is richer in olefins). Let us now formulate the optimum control actions which will be taken by the reactor controller after the feed disturbance enters S_1.

Optimizing Control Strategy for S_1. In Figure 9(a), the feasible region for S_1 is shown for the new values of disturbances when the recycle split s_r is kept at its optimal design value $s_r = 0.4647$. As it is clearly seen, the previous optimum design control policy where T_3 is regulated will lead to the violation of T_4. Therefore, T_3 is no more a control objective and a feasible point has to be determined.

Finding a Feasible Point and an Initial Search Direction (ISD). Starting from the point 1 which corresponds to the current set-point values of manipulated variables before disturbances have changed, there exist alternative ways to reach a feasible point F_0 as depicted in Figure 9(a). The route $1 \twoheadrightarrow 3 \twoheadrightarrow F_0$ is immediately screened out because it takes longer to recover feasibility. Let us study the control actions taken along each branch of the route $1 \rightarrow 2 \twoheadrightarrow F_0$.

Along $1 \rightarrow 2$.

s_1 = 0, quench valve to the first bed is closed
s_2 = continuously increased from $s_2 = 0$
s_3 = 0.6525
s_4 = continuously decreased from $s_4 = 0.3475$

The quench distribution shifts from the last bed to the second bed until at point 2, a new constraint is encountered: s_2 cannot be further increased since s_4 valve becomes fully closed, i.e., $s_4 = 0$. At point 2:

$s_1 = 0$, $s_4 = 0$, $s_2 = 0.3475$, $s_3 = 0.6525$, $s_4 = 0.4647$
T_3 = 909°R (505°K), T_4 = 946°R (525.6°K), Moles of Polymer: 39.0 mol/h

Point 2 is still not feasible with respect to T_4.

Along $2 \rightarrow F_0$.

We keep $s_4 = 0$ constraint tight and move along it by changing s_2 and s_3 together. It is important to note that starting from 1, the control action is first taken by the valves s_2 and s_4 to approach T_4 almost in a steepest ascent direction to the constraint surface. Later when T_4 is approached (i.e., point 2), fine valve adjustments are done by the valves s_2, s_3, s_3 taking over s_4, to exactly reach the feasible point F_0.

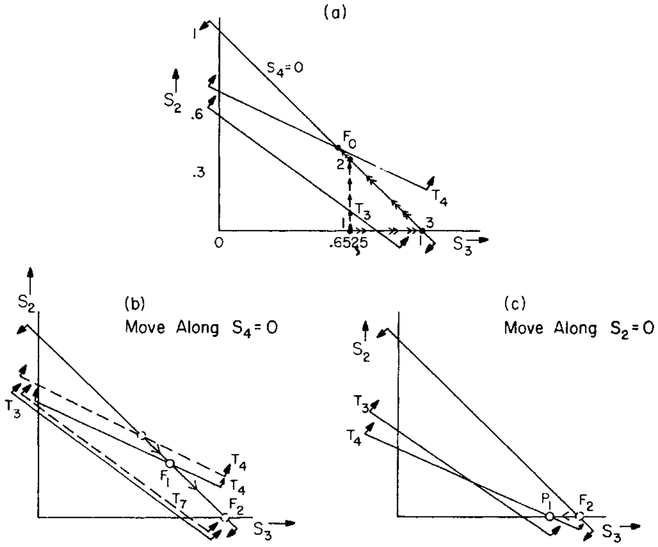

Figure 9. Dynamic evolution of the reactors' feasible region.

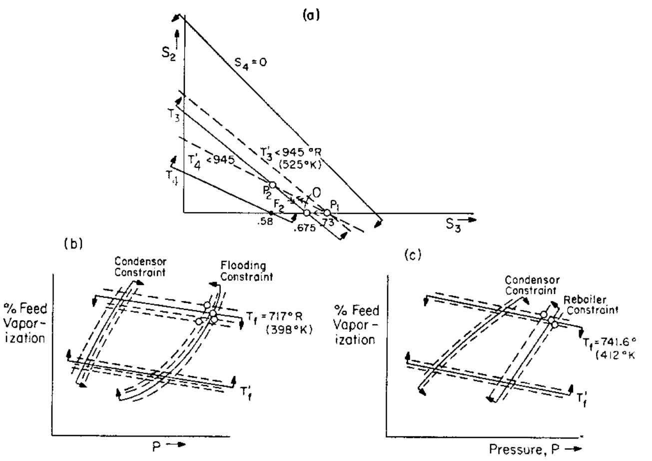

Figure 10. Alternative routes for the optimizing control of the reactors (a) and location of the optima for the depropanizer (b) and debutanizer (c) subsystems. – – – – location of constraints when $s_r = 0.52$. ——— location of T_4', T_3' constraints when quenches are set at their past optimum values with $s_r = 0.51$.

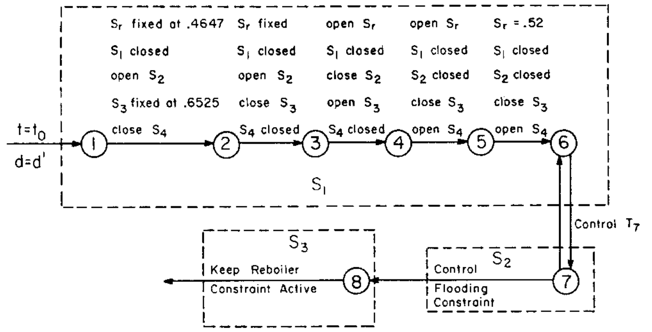

Figure 11. Sequencing for the polymerization plant for a feed composition disturbance.

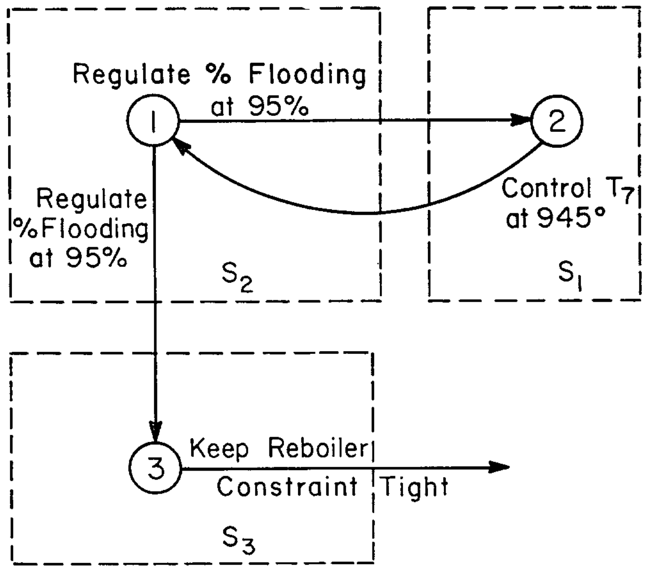

Figure 12. Sequencing for the plant for a propane recovery disturbance.

F_0 was also found to be the optimum for S_1 when the recycle split s_r is 0.4647. At F_0:

$s_2 = 0.41$, $s_3 = 0.59$, $s_4 = 0$
$T_3 = 907$°R (504°K), $T_4 = 945$°R (525°K), Moles of Polymer: 39.45 mol/h

The active temperature constraint T_4 is controlled by manipulating s_3. Up to now we applied ISD to arrive at a feasible point after the feed disturbances change. The sequence of quench valve adjustments was determined by the ISD for given recycle split s_r, i.e., its current design set-point. We will now start the search at F_0 towards the decentralized optimum of S_1 by changing s_r and finding the corresponding optimum quench distribution in the beds and repeating this search until the final optimum is achieved.

In Figure 9(b), it is shown that the optimum moves along the constraint $s_4 = 0$ for increasing s_r. The recycle quench flow is an interconnection input stream to the reactors. Therefore, the feasible region takes different shapes (i.e., T_3, T_4 constraints move) for different values of s_r's. Increase of recycle increases the conversion in the reactors as long as T_4 is regulated on its upper bound. Furthermore, optimal values continuously improve as one moves along $s_4 = 0$ in downhill direction.

After T_4 constraint hits the constraint $s_2 = 0$ at point F_2, further increase in recycle s_r moves the optimum along $s_2 = 0$ as shown in Figure 9(c). For example, for $s_r = 0.51$, the optimum is at:

$s_3 = 0.73$, $s_4 = 0.27$
$T_4 = 945$°R (525°K), Moles of Polymer: 40.44 mol/h

Along $s_2 = 0$, the active temperature constraints will change. For $s_r = 0.51$, T_4 is active whereas the final optimum, 0, T_3 will be active as shown in Figure 10(a). At the new optimum 0 for S_1, the manipulated and the dependent variables assume the following values:

$s_1 = s_2 = 0$, $s_3 = 0.675$, $s_4 = 0.325$, $s_r = 0.52$
$T_4 = 944$°R (524.5°K), $T_3 = 945$°R (525°K), Moles of Polymer: 40.4877 mol/h

Let us now examine how the optimizing control strategy is changed as we increase s_r from 0.51 to its optimum value 0.52 and as T_3 replaces T_4 as the active constraint. Figure 10(a) shows how the feasible region changes after the recycle split is increased to 0.52. Dashed lines indicate the values of the constraints T_3 and T_4, T_3' and T_4' after s_r is changed from 0.51 to 0.52, and the quench splits were kept at their previous optimum values for $s_r = 0.51$. After s_r is increased to 0.52, T_3' and T_4' remain in the feasible region and P_1 constitutes a feasible point from which alternative branches emanate towards the final optimum 0. Note that we do not continue controlling T_4 after s_r is increased since it will be infeasible with respect to T_3 as shown by point F_2.

Alternative Branches towards 0. Along the path $P_1 \rightarrow 0$, the quench to the third bed, s_3, is decreased which will increase T_3. At 0, s_3 cannot be further decreased since $T_3 = 945$°F (525°K) will be violated. At 0, T_3 is the primary variable to be controlled by manipulating s_3. Another alternative route is $P_1 \rightarrow P_2 \rightarrow 0$. Along $P_1 \rightarrow P_2$, movement is along $T_4 = T_4'$ which requires manipulation of the three quench valves s_2, s_3, s_4 (i.e., s_2 and s_4 increases, s_3 decreases). At P_2, T_3 becomes active and it is controlled at set-point $T_3 = 945$°R (525°K). Along $P_2 \rightarrow 0$, we move along $T_3 = 945$°R (525°K) which again requires manipulation of s_2, s_3 and s_4. This route will not be acceptable since it takes longer, and the production of polymer product is upset (i.e., along $P_1 \rightarrow P_2$ it decreases and along $P_2 \rightarrow 0$ it increases again). Therefore, the route $P_1 \rightarrow 0$ will identify the optimizing control actions necessary to reach the optimum.

Having established the optimizing control strategy for S_1, let us now examine the effect of the set-point changes of S_1 on the optimal operation of the second interconnected subsystem, i.e., the depropanizer. We start with examining how the feasible region of S_2 is affected by the interconnection inputs from S_1. Figure 10(b) demonstrates that the boundary of the feasible region remains the same and the optimum always lies along the flooding constraint. Therefore, the depropanizer optimizer will always regulate the tray load at its maximum limit 95% flooding as the reactor subsystem makes set-point changes and affects the depropanizer through the interconnection input. This simple feedback optimizing control strategy will guarantee both feasibility and optimality for the column.

As for the debutanizer subsystem, the optimum is always on the reboiler constraint independently of the values of interconnection inputs from the depropanizer subsystem as shown in Figure 10(c). The optimizing control policy of the third subsystem is simply to keep the steam pressure at its maximum value. This control action uniquely determines the column pressure and eliminates any open-loop feed forward pressure adjustments.

Figure 11 demonstrates the sequencing for the polymerization plant for a feed composition disturbance. Reactor's control actions are shown by a sequence of recycle and quench valve operations to control the active temperature constraints. Depropanizer controls the flooding constraint and the debutanizer keeps the reboiler constraint active in the face of varying interconnection inputs. The depropanizer dynamics are relatively slow compared to the reactor subsystem dynamics and there exist time lags between the two subsystems. Thus, the intensive properties of the interconnection input (i.e., quench recycle) from the depropanizer to the reactor have been assumed to be constant while set-point changes are accomplished in the reactor subsystem S_1 to reach its decentralized optimum. Once this optimum is achieved, it is maintained in the face of disturbances propagating from the depropanizer (see Figure 11).

B. The Effect of Propane Recovery Change. We will analyze the impact of a change in the propane recovery on the optimal operation of the overall plant. We consider a 1% decrease in the propane recovery as a disturbance for the depropanizer subsystem. At the new optimum for the depropanizer, the flooding constraint was again active where now the pressure increases to 380 psia (2600 kPa). The optimizing control action for the depropanizer is then to regulate the tray load in the stripping section. Control of the flooding constraint and the new recovery specification will uniquely determine the new steady-state value of the column overhead output, i.e., the interconnection input to the reactor subsystem. In response to this propagation of disturbance from the column to the reactor, the temperatures in the reactor will be regulated at their optimal set-points. At the optimum, T_3 is active and has to be controlled. For example, if T_3 is not controlled after the propane recovery decreases, the bed temperatures will be violated: T_3 = 945.7°R (525.4°K), T_4 = 945.8°R (525.5°K). This is due to the fact that there is less propane quench available when propane recovery decreases. Therefore, reactor optimizer will increase the recycle split s_r to keep T_3 active and achieve optimum operation:

s_r = 0.4695, T_3 = 945°R (525°K), T_4 = 944.9°R (525°K), Moles Polymer: 39.37 mol/h

Similarly, as the depropanizer bottoms product reaches its new steady-state value, debutanizer optimum is still at the reboiler constraint but now at a higher pressure. Debutanizer optimizing control action will be to keep its reboiler constraint active. The sequencing for the plant is illustrated in Figure 12.

C. Effect of Feed Flowrate Changes. As the last economic disturbance we consider a 10 mol/h feed flowrate increase. Development of the optimizing control structures and sequencing strategies follows the same procedure applied in feed composition disturbance case and details can be found in (Arkun, 1979).

SUMMARY

Optimizing control strategies for different subsystems of a gasoline polymerization plant were developed using constraint control approach. For all types of economic disturbances considered, the feasible region boundaries of the depropanizer and the debutanizer subsystems do not change and the optimal operations are always at the same constraints. Simple constraint control structures for these subsystems will lead to the optimal operation for both distillation columns, regardless of the disturbances. For the reactor subsystem, the third and fourth bed temperatures, T_3 and T_4 were found to be the critical constraints.

For the feasibility and optimality of the reactor operation, different optimizing control actions have to be taken depending on the type of disturbance. Those control actions were formulated in terms of the valve operations for the quench flows in order to develop a sequencing policy for the plant. During the development of the search strategy for the reactor subsystem, alternative routes resulted. These routes were screened based on the objective function behavior and the number of valve operations required for each route.

ACKNOWLEDGMENT

The financial support of the National Science Foundation through the Grant ENG75-11165-A01 is gratefully acknowledged.

APPENDIX

Representation of Interconnection Inputs in Terms of Optimizing Control Actions

At a steady-state operating point, we have the following active subsystem constraints

$$f_i(x_i, m_{iD}, \tilde{m}_i, u_i, d_i) = 0 \quad i = 1, \ldots, N \tag{A1}$$

$$c_i^p(x_i, m_{iD}, \tilde{m}_i, u_i, d_i) = c_{i,d}^p \quad dim(c_i^p) = dim(m_{iD}) \tag{A2}$$

$$dim(x_i) = dim(g_i)$$

and the interconnection constraints

$$u_i = \sum_{j=1}^{N} Q_{ij} y_j \tag{A3}$$

where

$$y_j = h_j(x_j, m_{jD}, \tilde{m}_j, u_j, d_j) \tag{A4}$$

Linear perturbations for Eq. A3 around an operating point gives for $i = 1, 2, \ldots, N$:

$$\delta u_i = \sum_{j=1}^{N} Q_{ij}\left(\frac{\partial h_j}{\partial x_j^T}\delta x_j + \frac{\partial h_j}{\partial m_{jD}^T}\delta m_{jD} + \frac{\partial h_j}{\partial \tilde{m}_j}\delta \tilde{m}_j + \frac{\partial h_j}{\partial u_j^T}\delta u_j + \frac{\partial h_j}{\partial d_j^T}\delta d_j\right) \tag{A5}$$

Similarly, from Eq. A1 one obtains

$$\delta x_j = -\left[\frac{\partial f_i}{\partial x_j^T}\right]^{-1}\left\{\frac{\partial f_j}{\partial m_{jD}^T}\delta m_{jD} + \frac{\partial f_j}{\partial \tilde{m}_j^T}\delta \tilde{m}_j + \frac{\partial f_j}{\partial u_j^T}\delta u_j + \frac{\partial f_j}{\partial d_j^T}\delta d_j\right\}$$
$$\equiv -J_i^{-1}M_{mD}\delta m_{jD} - J_j^{-1}\tilde{M}_j\delta\tilde{m}_j - J_j^{-1}U_j\delta u_j - J_j^{-1}D_j d_j \tag{A6}$$

Linear perturbations for Eq. A2 can then be written as:

$$\delta c_{jD}^p = \left(\frac{\partial c_j^p}{\partial m_{jD}^T} - \frac{\partial c_j^p}{\partial x_j^T}J_j^{-1}M_{jD}\right)\delta m_{jD} + \left(\frac{\partial c_j^p}{\partial \tilde{m}_j^T} - \frac{\partial c_j^p}{\partial x_j^T}J_j^{-1}\tilde{M}_j\right)\delta\tilde{m}_j + \left(\frac{\partial c_j^p}{\partial u_j^T} - \frac{\partial c_j^p}{\partial x_j^T}J_j^{-1}U_j\right)\delta u_j + \left(\frac{\partial c_j^p}{\partial d_j} - \frac{\partial c_j^p}{\partial x_j^T}J_j^{-1}D_j\right)\delta d_j$$
$$\equiv E_j\delta m_{jD} + F_j\delta\tilde{m}_j + G_j\delta u_j + H_j\delta d_j \tag{A7}$$

Solving for δm_{jD},

$$\delta m_{jD} = E_j^{-1}\delta c_{j,D}^p - E_j^{-1}F_j\delta\tilde{m}_j - E_j^{-1}G_j\delta u_j - E_j^{-1}H_j\delta d_j \tag{A8}$$

Substituting Eqs. A8 and A6 into Eq. A5 yields for $i = 1, 2, \ldots, N$.

$$\delta u_i = \sum_{j=1}^{N} Q_{ij}\left[\left(\frac{\partial h_j}{\partial \tilde{m}_j} - \frac{\partial h_j}{\partial x_j^T}J_j^{-1}\tilde{M}_j - \frac{\partial h_j}{\partial m_{jD}^T}E_j^{-1}F_j + \frac{\partial h_j}{\partial x_j^T}J_j^{-1}M_{jD}E_j^{-1}F_j\right)\delta\tilde{m}_j\right.$$
$$+\left(\frac{\partial h_j}{\partial u_j^T} - \frac{\partial h_j}{\partial x_j^T}J_j^{-1}U_j - \frac{\partial h_j}{\partial m_{jD}^T}E_j^{-1}G_j + \frac{\partial h_j}{\partial x_j^T}J_j^{-1}M_{jD}E_j^{-1}G_j\right)\delta u_j$$
$$+\left(\frac{\partial h_j}{\partial d_j^T} - \frac{\partial h_j}{\partial x_j^T}J_j^{-1}D_j - \frac{\partial h_j}{\partial m_{jD}}E_j^{-1}H_j + \frac{\partial h_j}{\partial x_j^T}J_j^{-1}M_{jD}E_j^{-1}H_j\right)\delta d_j$$

$$+\left(\frac{\partial h_j}{\partial m_{jD}^T} - \frac{\partial h_j}{\partial x_j^T} J_j^{-1} M_{jD}\right) E_j^{-1} \delta c_{jD}^p$$

$$\delta u_i \equiv \sum_{j=1}^{N} Q_{ij}[C_j \delta \tilde{m}_j + A_j \delta u_j + K_j \delta d_j + B_j \delta c_{jD}^p] \quad \text{(A9)}$$

Equation A9 can now be arranged to matrix equation

$$A\delta u = B\delta C_D^p + C\delta \tilde{m} + K\delta d \quad \text{(A10)}$$

or

$$\delta u = A^{-1}[B\delta C_D^p + C\delta \tilde{m} + K\delta d] \quad \text{(A11)}$$

where

$$\delta u = [\delta u_1, \ldots, \delta u_N]^T, \quad \delta C_D^p = [\delta C_{id}, \ldots, \delta C_{Nd}]^T,$$

$$\delta \tilde{m} = [\delta \tilde{m}_1, \ldots, \delta \tilde{m}_N], \quad \delta d = [\delta d_1, \ldots, \delta d_N]^T$$

and A, B, C, K are made up of submatrices:

$$A_{ij} \equiv \begin{cases} I - Q_{ii}A_i & i = j \\ -Q_{ij}A_j & i \neq j \end{cases}; \quad B_{ij} \equiv Q_{ij}B_j, \quad C_{ij} \equiv Q_{ij}C_j; \quad K_{ij} \equiv Q_{ij}K_j.$$

NOTATION

b_i = vector of upper bounds on inequality constraints
c_i^p = vector of primary controlled variables composed of active design constraints ($c_{i,opt}^p$) and regulatory control tasks ($c_{i,reg}^p$)
$c_{i,d}^p$ = vector of set-points for c_i^p
$\bar{c}_{i,opt}^p$ = the set of previously active constraints at X^* which remain active at X^o
$\tilde{c}_{i,opt}^p$ = the set of previously active constraints at X^* which become inactive at X^o
$c_{i,t}^p$ = vector of tight constraints
$c_{i,R}^p$ = vector of released constraints
$\tilde{c}_{i,R}$ = vector of controlled variables excluded from $c_{i,R}^p$ when new constraints ($\bar{g}_{i,IA}$) are encountered
$\bar{c}_{i,R}^p$ = new set of released constraints after $\tilde{c}_{i,R}^p$ is deleted from $c_{i,R}^p$
C_i = optimizing controller for S_i
d_i = vector of disturbances entering S_i
d_i^* = vector of disturbance design values
d_i' = vector of disturbance values after they have deviated from design values
f_i = subsystem system equations
g_i = subsystem design constraint functions
$g_{i,A}$ = vector of inactive subsystem constraints
$\bar{g}_{i,IA}$ = the set of previously inactive constraints which become active at a search point
$\tilde{g}_{i,IA}$ = the set of previously inactive constraints at X^* which remain inactive at X^o
$g_{i,k}$ = k^{th} inequality constraint in subsystem i
$h_i(\lambda)$ = subsystem dual function
$H(\lambda)$ = plant dual function
l_i = sub-Lagrangian
L = Lagrange function
m_i = vector of manipulated variables
$m_{i,j}$ = j^{th} component of m_i
$\tilde{m}_i$ = vector of extra free manipulated variables in S_i
$m_{i,D}$ = vector of manipulated variables controlling c_i^p
Q_i = incidence matrix denoting the interconnection among subsystems
r_i = regulatory control functions
$r_{i,d}$ = vector of design values for r_i
S_i = subsystem
u_i = vector of interconnection inputs
X^* = design optimum for the plant
X^o = feasible operating point for the plant
x_i = vector of state variables
y_i = vector of output variables

Greek Letters

β_i = vector of Kuhn-Tecker multipliers
λ_i = Lagrange multipliers for the interconnection constraints
Π_i = Lagrange multiplier for the disturbance specification $d_i - d_i' = 0$
Φ = overall plant objective (operating cost or operating profit)
Φ_i = subobjectives
∇ = gradient operator
δ = incremental changes

Subscripts

i = subscript used to denote the subsystem i
opt = to denote the controlled variables coming from optimization, i.e., active constraints
reg = to denote the controlled variables coming from regulatory control tasks
A = to denote active inequality constraints
IA = to denote inactive inequality constraints
T = to denote tight constraints
R = to denote released constraints
d = to denote desired values, i.e., set-points

LITERATURE CITED

Arkun, Y., "Design of Steady-State Optimizing Control Structures for Chemical Processes," Ph.D. Thesis, University of Minnesota (1979).

Arkun, Y. and G. Stephanopoulos, "Studies in the Synthesis of Control Structures for Chemical Processes: Part IV. Design of Steady-State Optimizing Control Structures for Chemical Process Units," *AIChE J.*, **26**, 975 (1980).

Barkelew, C. H., "Modern Process Control—State of the Art in Petroleum Refining," *Chemical Process Control*, AIChE Symp. Ser. 159, **72** (1976).

Baxley, R. A., "Local Optimizing Control for Distillation," *Instrumentation Technology*, p. 75 (Oct., 1969).

Davis, T. A., D. E. Griffin and P. U. Webb, "Cat Cracker Optimization and Control," *Chem. Eng. Prog.*, **70** (11), p. 53 (Nov., 1974).

DeBrosse, C. J. and A. W. Westerberg, "A Feasible-Point Algorithm for Structured Design Systems in Chemical Engineering," *AIChE J.*, **19** (2), p. 251 (1973).

Douglas, J. M., "Preliminary Process Design. Part III. Quick Estimates of Control Economics," AIChE Annual Meeting, New York (1977).

Duncanson, L. A. and P. V. Youle, "On-line Control of Olefin Plant," *Chemical and Process Engineering*, p. 49 (May, 1970).

Duyfjes, G. and P. M. E. M. Van Der Grinten, "Application of a Mathematical Model for the Control and Optimization of a Distillation Plant," *Automatica*, **9**, p. 537 (1973).

Ellingsen, W. R., "Implementation of Advanced Control Systems," *Chemical Process Control*, AIChE Symp. Ser. 159, **72** (1976).

Friedman, P. and K. L. Pinder, "Optimization of a Simulation Model of a Chemical Plant," *I & EC, Proc. Des. Dev.*, **11**, p. 512 (1972).

Gaines, L. D. and J. L. Gaddy, "University of Missouri-Rolla PROPS Users' Guide," Rolla, MO (1974).

Gaines, L. D. and J. L. Gaddy, "Process Optimization by Flowsheet Simulations," *I & EC, Proc. Des. and Dev.*, **15**, p. 206 (1976).

Govind, R. and G. J. Powers, "Control System Synthesis Strategies," AIChE 82nd National Meeting, Atlantic City, NJ (1976).

Ishida, C., "An Approach to Optimal Process Plant Operation," Japan-US Joint Seminar, Kyoto, Japan (June 23, 1975).

Joseph, B. and C. B. Brosilow, "Inferential Control of Processes. Part I.," *AIChE J.*, **24**, p. 485 (1978).

Kaiser, V. A., J. D. Mahoney, T. M. Stout, "An Optimum Approach to Optimization," ISA, 3.3-1-66 (Oct., 1966).

Kenney, W. F., "Reducing the Energy Demand of Separation Processes," *Chem. Eng. Prog.*, p. 68, (March, 1979).

Kuehn, D. R. and H. Davidson, "Computer Control II. Mathematics of Control," *Chem. Eng. Prog.*, **57** (6), p. 45 (June, 1961).

Lasdon, L. S., *Optimization Theory for Large Systems*, Macmillan Co. (1970).

Latour, P. R., "Comments on Assessments and Needs," *Chemical Process Control*, AIChE Symp. Ser. 159, **72** (1976).

Lee, W. and W. V. Weekman, Jr., "Advanced Control Practice in the Chemical Process Industry: A View from Industry," *AIChE J.*, **22**, (1976).

Maarleveld, A. and J. E. Rijnsdorp, "Constraint Control on Distillation Columns," *Automatica*, **6**, p. 51 (1970).

Morari, M., "Studies in the Synthesis of Control Structures of Chemical Processes," Ph.D. Thesis, University of Minnesota (Dec., 1977).

Morari, M., Y. Arkun and G. Stephanopoulos, "An Integrated Approach to the Synthesis of Process Control Structures," JACC Proceedings, Philadelphia, PA (1978).

Morari, M., Y. Arkun and G. Stephanopoulos, "Studies in the Synthesis of Control Structures for Chemical Processes. Part I. Formulation of the Problem. Process Decomposition and the Classification of the Control Tasks. Analysis of the Optimizing Control Structures," *AIChE J.*, **26**, p. 220 (1980a).

Morari, M. and G. Stephanopoulos, "Studies in the Synthesis of Control Structures for Chemical Processes. Part II. Structural Aspects and the Synthesis of Alternative Feasible Control Schemes," *AIChE J.*, **26**, p. 232 (1980b).

Morari, M. and G. Stephanopoulos, "Studies in the Synthesis of Control Structures for Chemical Processes. Part III. Optimal Selection of Secondary Measurements Within the Framework of State Estimation in the Presence of Persistent Unknown Disturbances," *AIChE J.*, **26**, p. 247 (1980c).

Motard, R. L., H. M. Lee, R. W. Barkeley, D. M. Ingels, *CHESS, Chem. Eng. Simulation System: System's Guide*, Technical Publ. Co., Houston, TX (1968).

Prett, D. M. and R. D. Gillette, "Optimization and Constrained Multivariable Control of a Catalytic Cracking Unit," 86th National AIChE Meeting (April, 1979).

Rijckaert, M. J., Martens, X. M. and J. Desarnauts, "Ethylene Plant Optimization by Geometric Programming," *Computers in Chem. Eng.*, **2**, p. 93 (1978).

Rijnsdorp, J. E., "Chemical Process Systems and Automatic Control," *Chem. Eng. Prog.*, **63** (7), p. 97 (July, 1967).

Rivas, J. R., D. F. Rudd and L. R. Kelly, "Computer-Aided Safety Interlock Systems," *AIChE J.*, **20** (2), p. 311 (1974).

Roffel, B., H. J. Fontein, "Constraint Control of Distillation Processes," *Chem. Eng. Sci.*, **34**, p. 1007 (1979).

Shah, M. J. and R. E. Stillman, "Computer Control and Optimization of a Large Methanol Plant," *Ind. and Eng. Chemistry*, **62** (12), p. 59 (Dec., 1970).

Umeda, T. and T. Kuriyama, "A Logical Structure for Process Control System Synthesis," Proc. of IFAC Congress, Helsinki, Finland (1978).

Webb, P. U., B. E. Lutter and R. L. Hair, "Dynamic Optimization of FCC Units," AIChE Annual Meeting, New York (1977).

Weber, R. and C. Brosilow, "The Use of Secondary Measurements to Improve Control," *AIChE J.*, **18**, p. 614 (1972).

Westerberg, A. W., "Decomposition Methods for Solving Steady-State Process Design Problem," in *Decomposition of Large-Scale Problems*, ed., D. M. Himmelblau, North Holland Pub. Co. (1973).

Westerberg, A. W. and C. J. DeBrosse, "An Optimization Algorithm for Structured Design System," *AIChE J.*, **19**, p. 335 (1973).

Wismer, D. A., ed., *Optimization Methods for Large-Scale Systems . . . with Applications*, McGraw-Hill (1971).

Manuscript received October 5, 1979; revision received August 14, and accepted August 20, 1980.

Design of Advanced Process Controllers

This paper deals with defining the relation between modeling of process units and controller design. In the process industries, it is often difficult to obtain accurate process models. It is shown that advanced algorithms such as dead-time compensators require more detailed process information for design than do with *PI* and *PID* controllers. A method is described to systematically evaluate the relation between process identification and controller design, stability, and performance. It is shown that conventional gain and phase margins do not provide proper safety margins for dead-time compensators and optimal controllers. Methods for safe design of dead-time compensators are derived, and the approach could be useful in a wide class of problems.

To illustrate the approach presented, the design of *PI* controllers by conventional methods is analyzed. The conditions, as well as the exceptions, are specified in which methods such as described by Ziegler and Nichols or Cohen and Coon will give good results. It is shown that for any stable nonlinear system with an input/output function $y = G_p^*(u)$, a linearized design function G'_{pd} can be constructed and identified that guarantees stability and reasonable performance of the controller (Eqs. 21 and 22 and Figures 4-7) over a wide range of operating conditions. A rigorous framework for identifying the exceptions and understanding the reason why such methods work is presented.

Z. J. PALMOR

Mechanical Engineering, Technion Israel Institute of Technology Haifa, Israel

and

R. SHINNAR

Chemical Engineering Department City College of New York New York, NY

SCOPE

The paper deals with a fundamental problem of chemical engineering design, the relation between the quality of the information required for a specific design and the performance of the system. Chemical process units are normally nonlinear systems, the exact mathematical description of which is complex and difficult to obtain. We therefore have to ask ourselves what is the type and accuracy of information really required for a specific design problem and how much will better information pay off in increased performance. Here, we try to approach this question for continuous controllers with a single measured and manipulated variable, starting with simple *PI* controllers and then looking at control loops incorporating a dead time compensator.

The emphasis is not on tuning recipes, but on trying to understand how strongly simplified linearized models permit design of controllers for nonlinear complex systems and to define the quality of the information required for design in a rigorous way. The approach taken uses the concept of model space defined in a previous paper. It is explained in detail with a few examples and related to present methods of controller design. It should be a useful tool in a number of other applications in chemical reactor design as well as in the design of control systems in general.